INTERNATIONAL JOURNAL OF HYDROGEN ENERGY 41 (2016) 8992–9003

Available online at www.sciencedirect.com

ScienceDirect

journal homepage: www.elsevier.com/locate/he

Fatigue properties of catalyst coated membranes for fuel cells: Ex-situ measurements supported by numerical simulations

R.M.H. Khorasany, Y. Singh, A. Sadeghi Alavijeh, E. Kjeang[*], *G.G. Wang, R.K.N.D. Rajapakse*

Fuel Cell Research Laboratory (FCReL), School of Mechatronic Systems Engineering, Simon Fraser University, 250-13450 102 Avenue, Surrey, BC V3T 0A3, Canada

ARTICLE INFO

Article history:
Received 18 December 2015
Received in revised form
21 March 2016
Accepted 6 April 2016
Available online 27 April 2016

Keywords:
Fuel cell
Membrane
Catalyst layer
CCM
Fatigue

ABSTRACT

The interactions between catalyst layers and membrane are known to have significant impact on the mechanical properties of the composite catalyst coated membrane (CCM) materials used in fuel cells. The mechanical fatigue durability of such composite CCM materials is investigated herein, and compared to the characteristics of pure membranes. Ex-situ uniaxial cyclic tension tests are conducted under controlled environmental conditions to measure the fatigue lifetime, defined by the number of stress cycles that the specimen can withstand before mechanical failure. The sensitivity of the CCM fatigue lifetime to the applied stress is determined to be higher than that of the pure membrane, and varies significantly with environmental conditions. The experimental results are then utilized to develop a finite element based CCM fatigue model featuring an elastic–plastic constitutive relation with strain hardening. Upon validation, the model is used to simulate the fatigue durability of the CCM under cyclic variations in temperature and relative humidity, which is critical for fuel cells but cannot be effectively measured ex-situ. When combined, the experimental and numerical methods demonstrated in this work provide a novel, convenient approach to determine the CCM fatigue durability under various hygrothermal loading conditions of relevance for fuel cell design and operation.

Introduction

The polymer electrolyte fuel cell (PEFC) is a promising technology for generation of electricity with zero emissions at the point of use [1,2]. The widespread use of this clean technology is currently hindered by its low durability and high costs associated with producing the fuel cell stacks [1]. Two broad and general causes are responsible for the membrane degradation phenomena often associated with PEFC failure: chemical and mechanical degradation. Hydrogen peroxide decomposition in the membrane creates radicals that chemically degrade the ionomer [3–8]. Furthermore, it is noted that the mechanical properties such as strain to failure and stress–strain relation are highly affected by the chemical degradation [9,10]. So far, most of the scholarly work in the

* *Corresponding author*. Tel.: +1 778 782 8791; fax: +1 778 782 7514.
E-mail address: ekjeang@sfu.ca (E. Kjeang).
http://dx.doi.org/10.1016/j.ijhydene.2016.04.042

area of PEFC durability has been focused on the chemical degradation mechanisms [1,11–13].

Along with the chemical degradation, the mechanical degradation phenomena can be an equally critical degradation mode for PEFC membranes [14]. An essential step toward understanding the mechanical membrane degradation process is to first understand the basic membrane behavior under different levels of hygrothermal and mechanical loading conditions [15]. Previous experimental investigations have revealed that ionomer membranes exhibit a predominantly linear viscoelastic stress–strain behavior below the yield point [9–11] and a nonlinear plastic response with strain hardening above the yield point [17]. Moreover, the stress–-strain characteristics of the membrane are highly dependent on the environmental conditions of temperature and humidity [18–21] and may also depend on the loading rate [22]. Based on these characteristics, several numerical finite element models have been suggested for the mechanical behavior of the membrane [16,22–27]. These models have been employed to simulate both ex-situ and in-situ responses of the membrane under hygrothermal and mechanical loading conditions [28–35].

Previous research on the mechanical degradation behavior of ionomer membranes can be divided into three main categories: (i) fracture; (ii) fatigue; and (iii) creep. Fuel cell membranes are prone to creep when subjected to periods of high stress, depending on confinement within the membrane electrode assembly [36,37]; however, membrane failure is generally associated with hydrogen leak bearing fractures. The fracture resistance property has been used as an indicator of the mechanical durability of cracked membranes [38,39]. Additionally, the fracture characteristics of the membrane were reported to be time dependent regardless of the level of relative humidity or temperature [40]. Crack evolution and delamination between the catalyst layers and membrane can be influenced by both external mechanical vibrations and by cycling of internal stresses due to hygrothermal variations [41,42]. However, it should be emphasized that the mechanical and chemical degradation phenomena are generally coupled during fuel cell operation [8,43–45], which may further complicate the process.

In the absence of chemical degradation, fracture development in fuel cell membranes is normally driven by the underlying mechanical fatigue phenomena when the material is subjected to cyclic hygrothermal and mechanical loadings due to dynamic hydration and dimensional changes of the ionomer [46]. These cyclic loadings are known to cause initiation and propagation of microcracks inside the membrane [47,48], which may grow into macroscopic fractures. In-situ simulation results have suggested that during a typical hygrothermal fluctuation, the stress and strain alternate between tensile and compressive states [26]. In addition, a considerable amount of plastic strain can be generated in the membrane at elevated levels of temperature and relative humidity [24], which can influence the fatigue fracture process [49]. The fatigue lifetime of the membrane is not only affected by the amplitude of the mechanical or hygrothermal fluctuations but also depends upon the environmental conditions [47]. Ex-situ measurements have revealed that the fatigue lifetime of the membrane increases exponentially with decreasing amplitude of cyclic mechanical loading [47,49,50]. Cyclic mechanical and hygrothermal loadings were shown to reduce the strain to failure of the membrane although the Young's modulus was intact [51]. However, it has also been reported that hygrothermal aging may increase the elastic modulus and tensile strength [52].

Experimental techniques utilizing cyclic mechanical forces have been suggested as a primary tool for studying the effects of cyclic loading on the mechanical fatigue lifetime of the membrane [47,49]. However, such approaches are generally limited to application of mechanical stress cycles rather than hygrothermal cycles. Alternatively, numerical methods provide more flexible and less expensive tools for similar purposes [23,53]. Most existing numerical models have concentrated on predicting the membrane lifetime at its most critical point [54] and rely on empirical relations. Recently, Khorasany et al. [48] developed a finite element based numerical model capable of simulating the ex-situ fatigue lifetime of pure membranes under a wide range of environmental conditions relevant for fuel cell applications. Compared to the previous works, this model provided an additional capability of predicting the spatial distribution of the fatigue lifetime within the membrane domain.

In most PEFCs, the membrane is coated with anode and cathode catalyst layers on each side to form a catalyst coated membrane (CCM). The membrane and the two catalyst layers collectively constitute a composite material bonded through the common ionomer phase with its mechanical properties significantly different from those of the pure membranes [46,55]. Therefore, the fatigue behavior of the membrane is also expected to differ when situated within a CCM. Previous research using pressure-loaded biaxial blister testing has indicated that the mud-cracks in the catalyst layers may have a negative effect on the mechanical stability of the membrane [50]. The presence of contaminants such as foreign cations and chlorides and high humidity conditions were found to have deleterious effects on the fracture resistance of CCMs [56].

While the mechanical properties and degradation mechanisms of pure ionomer membranes are relatively well-established, the more complex mechanical degradation process of the composite CCM is not yet well understood. Hence, the first objective of the present work is to develop a fundamental understanding of the fatigue behavior of the CCM under a wide range of conditions that mimic the fuel cell environment. Ex-situ fatigue experiments are therefore designed to investigate the effect of cyclic mechanical loadings on the CCM fatigue lifetime under controlled environmental conditions. The results obtained are then compared against the corresponding data for pure membranes in order to determine the effect of the catalyst layers on the mechanical stability of the CCM. The second main objective of this work is to use the experimental data to develop and validate a finite element based model for CCM fatigue simulation. The model is then applied to analyze the effect of cyclic hygrothermal loadings on the ex-situ fatigue lifetime of the CCM, which is more relevant for fuel cell operation. The detailed analysis conducted in this work is expected to enhance the fundamental understanding of fatigue-induced mechanical degradation in the context of overall PEFC durability.

Experimental technique

Materials

The CCM material used in this work was based on a Nafion® NR-211 membrane, which is a 25 μm thick perfluorosulfonic acid (PFSA) ionomer membrane commonly applied in PEFCs and previously used in our membrane fatigue research [47]. The catalyst layers of the CCM were made of Pt/C and PFSA ionomer and had a thickness comparable to that of the membrane [47,48]. To satisfy the consistency requirements, the CCM samples were kept in room conditions for several days before testing. Custom-designed dies of the dogbone shape shown schematically in Fig. 1 were used to cut specimens for ex-situ testing. The CCM sheets were placed on a plate made of tool steel and the dies were pressed against the sheet using a hydraulic press. To make consistent cuts and avoid cutting deficiencies, a thin piece of paper was placed on top of the CCM sheet. The CCM specimens were regularly checked using an optical microscope to ensure cutting accuracy.

Test procedure

Tensile fatigue experiments were conducted using a dynamic mechanical analyzer (TA Instruments Q800 DMA) equipped with temperature and humidity control. The CCM specimens were mounted in the tensile clamp of the DMA at room conditions and placed under a small preload force (0.001–0.005 N) to keep the specimen under tension during the test initiation. To avoid stress concentration in the central section of the specimen, the DMA grips were only allowed to cover the rectangular end lobes on each side. The temperature and relative humidity were elevated from room conditions to the desired pre-set values during which the lengthwise specimen elongation was monitored. The specimen was held under the desired elevated temperature and relative humidity conditions for at least 30 min to ensure adequate equilibration in the final specimen length before testing. A dynamic force profile consisting of a mean, constant force (P) and an oscillating, sinusoidal force was then applied. The frequency of the sinusoidal load was 10 Hz. The amplitude of the dynamic force contribution was such that the minimum to maximum engineering stress ratio in the central part of the specimen was 0.2 [47,49]. Due to the dynamic loading conditions, microcracks were expected to initiate in the specimen over time [57]. Once the density of the microcracks exceeds a certain limit beyond which the specimen can no longer withstand the dynamic force, a sudden mechanical rupture occurs [49]. Accordingly, the CCM fatigue lifetime was measured in terms of the number of stress cycles from the start of the dynamic force application until the final failure of the specimen [47].

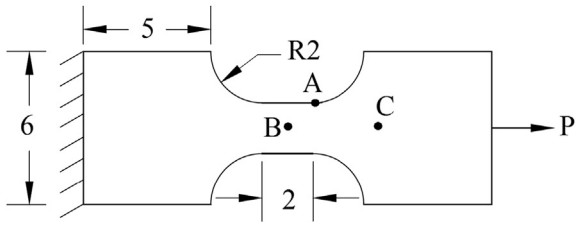

Fig. 1 – Schematic of the dogbone shaped CCM specimen geometry used in the present experiments (all dimensions are in mm). Points A, B, and C indicate the points of interest analyzed in the modeling work.

The stresses applied in the experiments should represent those experienced by the CCM under in-situ conditions. The CCM has time-dependent characteristics due to which the mechanical response changes with the loading rate [33]. Additionally, due to the stress relaxation behavior of the membrane inside the CCM, the stress amplitude decreases with time [24,26,58]. Mechanical fatigue is a dynamically driven phenomenon, meaning that the effect of the dynamic stress amplitude is stronger than the effect of the mean stress. Hence, when the stress range is selected, it is important to consider the pre-relaxation peak values of the stress [26]. Our previous work has indicated that when the CCM is treated as a composite material, the membrane experiences a smaller amplitude of stress oscillations compared to the case where the membrane and catalyst layers are treated separately [33]. Moreover, the fuel cell geometry can substantially change the stress profile inside the membrane [59]. In-situ accelerated stress tests have shown membrane lifetimes under cyclic hygrothermal loadings below one million cycles [60]. Therefore, the stress levels in the experiments should be selected such that the membrane fatigue lifetime does not exceed what can be practically achieved during real operating conditions [47]. Here, a range of maximum engineering stress levels of 1–5 MPa was selected, which corresponds to failure in less than one million cycles. These stress levels are substantially lower than those used previously for pure membrane testing [33,55], and are adjusted depending on the environmental conditions according to the tensile properties of the CCM.

A design of experiments analysis was conducted based on a 2^2 factorial experiment in order to determine the effects of relative humidity and temperature on the CCM fatigue lifetime and the maximum stress level. The two factors (relative humidity and temperature) were jointly varied across four sets of environmental conditions relevant to fuel cell applications from room conditions (23 °C, 50% RH) to fuel cell operating conditions (70 °C, 90% RH). The other remaining corners in the design matrix were: 23 °C, 90% RH and 70 °C, 50% RH. At least three specimens were tested at each set of environmental conditions. The significance of the statistical effects of the relative humidity and temperature was evaluated using a standard F-test based analysis of variance (ANOVA) method [47].

Experimental results

Tensile fatigue durability experiments were conducted under a wide range of applied stress levels and environmental conditions in order to map out the fatigue properties of the CCM and compare them against the previously measured membrane properties. The measurements were conducted using a fixed minimum to maximum stress ratio of 0.2 in all cases,

implying that the mean stress and stress amplitude were jointly altered. The CCM fatigue lifetime and plastic strain were measured at each loading condition [47].

S–N curves

The obtained CCM fatigue lifetime (N) versus the maximum engineering stress (S) at different environmental conditions is presented on a logarithmic scale in Fig. 2. As can be seen from this figure, the CCM fatigue lifetime increases exponentially as the applied maximum stress is reduced, which is a common material characteristic that is qualitatively consistent with the previously measured membrane results [47]. At a given lifetime, the maximum tolerable stress level is observed to drop when the relative humidity is elevated from room condition to 90%. This is corroborated by the softening effect of the material under elevated environmental conditions [55]. At elevated levels of temperature, the drop in the maximum stress level is even more pronounced. This is again attributed to the softening of the yield point and post yield behavior of the material which is more profound at elevated temperature than at elevated humidity within the currently tested range [55].

A comparison of the present CCM results to the previously reported fatigue data for pure membranes [47] indicates a relatively similar overall fatigue behavior. However, the maximum stress levels that the CCM can withstand before the final rupture are substantially lower than for the membrane. This is primarily attributed to the lower mechanical strength of the catalyst layers compared to the membrane, resulting in a composite CCM material that is weaker than a pure membrane [20,55]. Additionally, due to lower elastic modulus and post yield tangent modulus of the CCM material, the CCM fatigue lifetime is more sensitive to the changes in the stress value [33].

An ANOVA analysis was conducted to quantify the effects of temperature and relative humidity on the stress levels required to achieve specific fatigue lifetimes (2×10^5, 4×10^5, 6×10^5, and 8×10^5 cycles). The key results are summarized and compared to previous data for pure membranes in Table 1 [47]. The p values were consistently small (<0.001), indicating that all

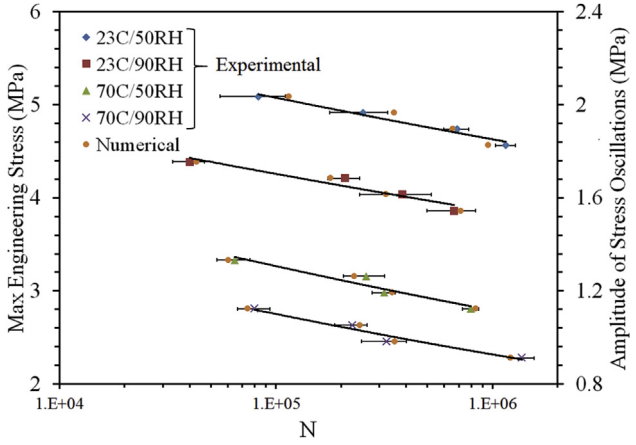

Fig. 2 – Measured and simulated fatigue life curves in the form of maximum engineering stress (S) and amplitude of engineering stress oscillations versus the number of cycles to failure (N).

effects were statistically significant. Similar to the pure membrane results, the temperature and relative humidity had negative main effects on the maximum stress levels for the CCM, which means that the stress decreased with increasing levels of temperature and humidity. This is due to the softening effect at elevated levels of relative humidity or temperature. The main effect of temperature was substantially stronger than that of the humidity. However, the interaction (or combined effect) of the relative humidity and temperature increased the stiffness of the CCM [55]. Therefore, the interaction of these two factors had a positive effect on the maximum stress level. Previous experimental results have revealed that the CCM material yields at lower stress levels than the pure membrane. Additionally, the post yield tangent modulus of the CCM is significantly lower than that of the membrane [55]. As a result, the effects of the relative humidity and temperature factors on the maximum stress levels are less pronounced for the CCM than for the membrane. It is also noteworthy that the temperature, relative humidity, and interaction effects of the CCM material experienced merely small changes with respect to the fatigue lifetime. Considering that these changes are within a few percent of the overall effects, it can be concluded that the present findings are valid for a wide range of fatigue lifetimes. Overall, the obtained fatigue durability closely resembles the tensile strength behavior of the CCM material: a high tensile strength appears to give high fatigue durability under the measured conditions.

Strain characteristics

The strain to failure of the CCM material plays an important role in its fatigue durability when subjected to cyclic mechanical or hygrothermal loadings. The experimental results for the true strain to failure of the CCM specimens subjected to cyclic loading are presented in Fig. 3. Due to the softening effect, the strain to failure of the CCM is considerably higher at elevated levels of relative humidity and temperature conditions than at room conditions. Moreover, a marginal increase in final strain is observed with increasing maximum stress in all cases. However, this change is negligible compared to the natural variability of the experiment. It is noteworthy that the elongation of the CCM during fatigue testing is considerably lower than that of the pure membrane [47] despite the higher applied mean force required to reach the same internal stress level. This result confirms the reinforcing effect of the catalyst layers, but also reveals that the CCM may fail earlier than the membrane at a lower level of strain [55]. Optical images of the surface of the CCM [61,55] have shown that severe cracks are initiated in the catalyst layers when the CCM is subjected to stresses above the yield point. In the presence of catalyst layer cracks, the forces previously supported by these layers will be transferred to the membrane part of the CCM, which results in the failure of the CCM at lower strains compared to the pure membrane [47].

Numerical model

Although experiments are useful tools in understanding the fatigue behavior of the CCM material, they have their own

Table 1 – ANOVA results for the maximum stress corresponding to specific fatigue lifetimes (N) of the CCM and membrane [47]. The main effects of temperature and relative humidity as well as their interaction effect are given in units of MPa.

	Temperature		Relative humidity		Interaction	
	CCM	Membrane	CCM	Membrane	CCM	Membrane
$N_1 = 2 \times 10^5$	−1.64	−6.99	−0.67	−2.08	0.16	0.72
$N_2 = 4 \times 10^5$	−1.68	−6.96	−0.64	−1.92	0.15	0.83
$N_3 = 6 \times 10^5$	−1.70	−6.94	−0.62	−1.83	0.14	0.88
$N_4 = 8 \times 10^5$	−1.72	−6.92	−0.61	−1.77	0.13	0.92

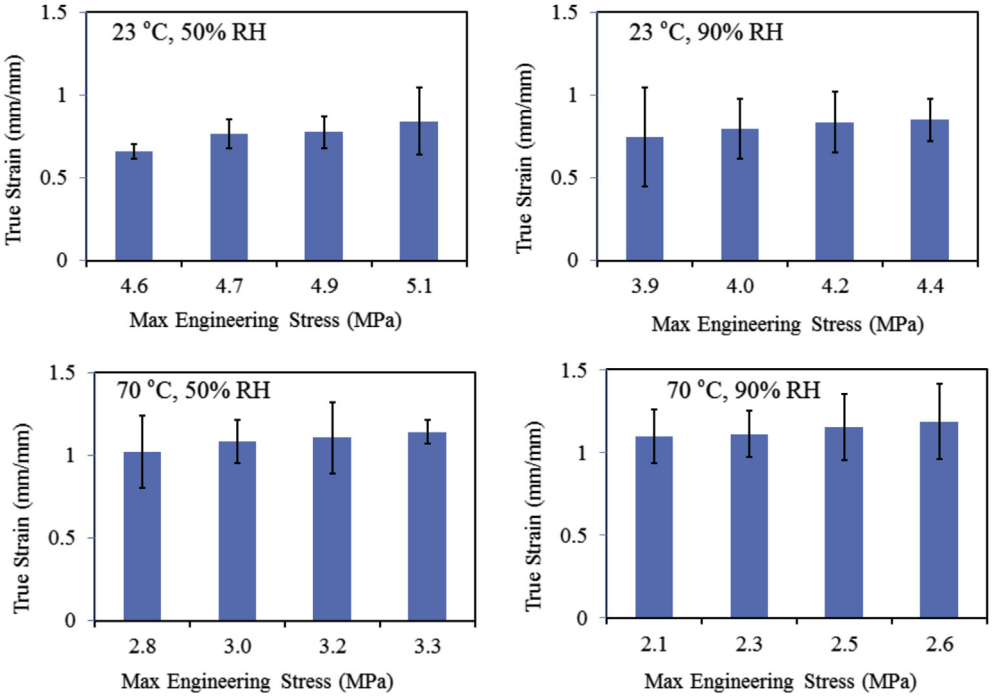

Fig. 3 – Final true strain of the CCM at four different environmental conditions.

limitations. Most notably, experiments involving cyclic hygrothermal oscillations are either very expensive or practically impossible to facilitate in a reasonable timeframe. Conducting in-situ experiments under real-time cyclic hygrothermal loading conditions is even more challenging. Therefore, finite element based modeling often provides a more productive and less costly method to simulate fatigue lifetime. Here, the finite element method was utilized to predict the CCM fatigue lifetime for a wide range of hygrothermal loading conditions relevant to fuel cell operation [48].

Previous experimental investigations [55] suggest that the response of the CCM is approximately linear elastic up to the yield point. Hence, for strains below the yield point, the linear relation between stress and elastic strain is described by Hooke's law:

$$\sigma_{ij} = \frac{E}{(1+\upsilon)(1-2\upsilon)}\left[\upsilon\varepsilon^e_{kk} + (1-2\upsilon)\varepsilon^e_{ij}\right] \quad i,j,k = 1,2,3 \tag{1}$$

where σ_{ij} represents the components of true stress; ε^e_{ij} represents the components of elastic strain; E is Young's modulus; υ is Poisson's ratio; and $\varepsilon^e_{kk} = \varepsilon^e_{11} + \varepsilon^e_{22} + \varepsilon^e_{33}$. At each environmental condition, the Young's modulus and Poisson's ratio were experimentally obtained from our previously reported data [33,55]. The incompressible nonlinear post yield response of the CCM is characterized using plastic flow according to the von Mises yield function:

$$\begin{aligned} f(\sigma_{ij}) &= \sqrt{\frac{3}{2}S_{ij}S_{ij}} - \sigma_y \\ \sigma_{kk} &= \sigma_{11} + \sigma_{22} + \sigma_{33} \\ S_{ij} &= \sigma_{ij} - 1/3\sigma_{kk}\delta_{ij} \end{aligned} \tag{2}$$

where σ_y is the yield stress and S_{ij} represents the components of the deviatoric stress. The yield stress of the CCM was considered to be a function of the relative humidity (RH), temperature (T), and plastic strain as follows [55]:

$$\sigma_y = \sigma_y(\varepsilon^p, T, RH) \tag{3}$$

where ε^p is the current equivalent plastic strain defined by:

$$\varepsilon^p = \int \sqrt{\frac{2}{3}d\varepsilon^p_{ij}d\varepsilon^p_{ij}} \tag{4}$$

According to this model, yield occurs when the yield function is $f = 0$. The material exhibits plastic behavior when $f > 0$ and deforms elastically when $f < 0$.

The CCM fatigue lifetime is mainly affected by the amplitudes and mean values of stress and strain oscillations, as shown experimentally in the previous section. To account for both stress effects, the Smith-Watson-Topper (SWT) model was used [62–64] which is mathematically represented as follows:

$$\sigma_{max}\frac{\Delta\varepsilon}{2}=\frac{(\sigma'_f)^2}{E}(2N_f)^{2b}+\sigma'_f\varepsilon'_f(2N_f)^{b+c} \quad (5)$$

where σ_{max} is the maximum stress; $\Delta\varepsilon$ is the amplitude of the strain oscillations; σ'_f is the fatigue strength coefficient; b is the fatigue strength exponent; N_f is the fatigue lifetime; ε'_f is the fatigue ductility coefficient; and c is the fatigue ductility exponent.

Simulation results

The fatigue model described by Equations (1)–(5) was numerically applied to the specimen geometry in Fig. 1 to simulate the response of the CCM material under the application of cyclic hygrothermal loadings. The simulations were conducted using the finite element based software COMSOL Multiphysics® version 4.3. A 2D meshing scheme was adopted in the simulations. The governing equations of motion used here were based on the mechanical equilibrium equations in the relevant spatial directions. The boundary conditions were chosen to replicate the experimental configurations (fixed displacement at the left end, sinusoidal stress at the right end, and remaining boundaries kept free). The nonlinear solver of COMSOL based on the iterative solution schemes was adopted to solve the associated equilibrium equations with boundary conditions. The material properties were obtained from the experimental results and are summarized in Table 2.

Model validation

To examine the correctness and accuracy of the new CCM fatigue model, the specimen geometry shown in Fig. 1 was first used to simulate the mechanical fatigue lifetime of the CCM under cyclic mechanical loadings at fixed environmental conditions. It was assumed that one end of the specimen is clamped and a cyclic mechanical loading with a nonzero mean value is applied to the other end. The obtained fatigue lifetime distribution within the CCM specimen under the fuel cell environmental condition is presented in Fig. 4, based on two representative stress levels. The stress and strain, which are point functions, were first calculated at each point within the specimen geometry by the finite element simulations. Thereafter, the stress and strain dependent fatigue lifetime was evaluated independently for each point. This enables the generation of spatial distribution of lifetime graphs, such as Fig. 4, which aid in the identification of regions that are most likely to experience fatigue induced failure. The fatigue lifetime is expressed as the logarithmic number of cycles that the material can withstand before mechanical failure due to fatigue, which is now a function of position within the specimen. As the accuracy of the simulation results is not experimentally verifiable beyond 10^7 cycles, the regions with lifetimes higher than this threshold are shown to have 10^7 cycles. Due to the strain and stress concentration effects, the CCM lifetime is shown to have a global minimum at the four corner points (Point A in Fig. 1) at the edge of the central section of the specimen. This coincides with the experimental observations where the primary location for specimen failure was in the vicinity of these corner points. The fatigue lifetime at the two rectangular end lobes is shown to be longer than in the central section due to lower stress values and associated lower strain amplitude resulting from the dogbone geometry.

A series of fatigue lifetime simulations were conducted under a range of environmental conditions relevant to fuel cell applications in order to comprehensively validate the numerical model. The applied static and dynamic force profiles were identical to those used for the experimental investigations. For comparative purposes, the fatigue lifetime was taken at the point with the minimum lifetime (Point A), i.e., the point of failure. A thorough comparison between the numerical findings and the experimental data (shown in Fig. 2) indicated a good agreement between the experimental data and the simulated results at all environmental conditions, which validates the fatigue model and justifies its use in carrying out further case studies to develop a better understanding of the fatigue phenomenon in CCMs. It should be noted that the simulations in this work are specifically

Table 2 – CCM fatigue material constants at four different environmental conditions.

	σ'_f (MPa)	b	ε'_f	c
23 °C, 50% RH	5.75	−0.0435	0.9	−0.7
23 °C, 90% RH	4.98	−0.0422	0.9	−0.7
70 °C, 50% RH	4.99	−0.0696	0.9	−0.7
70 °C, 90% RH	4.7	−0.0745	0.9	−0.7

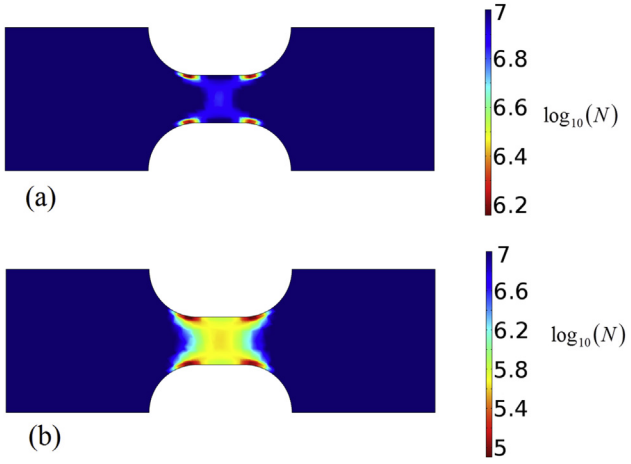

Fig. 4 – Spatial distribution of simulated fatigue lifetime within the CCM specimen under cyclic mechanical loadings at the fuel cell environmental condition (70 °C, 90% RH) with an applied maximum engineering stress of (a) 2.3 MPa and (b) 2.8 MPa. The lifetime values given by the number of stress cycles until failure (N) are presented on a logarithmic scale. Lifetimes exceeding 10^7 cycles are not shown.

focused on ex-situ applications where out of plane stresses are neglected. This enables validation of the chosen modeling approach (SWT) and the solver (COMSOL) against experimental results which are also ex-situ. Moreover, the in-plane stresses used in the ex-situ simulations are of the same order of magnitude as those predicted by previous in-situ numerical studies [33], and by using those stresses, the developed model can be extended for in-situ applications as well.

Simulated fatigue lifetime under hygrothermal loading

In our previous work, it was found that the fatigue lifetime of a pure membrane is substantially affected by the amplitudes of the temperature and relative humidity stressors and the mean applied nominal stress during cyclic hygrothermal loadings [48]. In the present CCM case, the effect of the applied nominal stress was first investigated followed by the effect of the temperature and relative humidity amplitudes on the fatigue lifetime of the CCM. Simulations conducted in this section were based on the assumption that the sample is vertically constrained at the two end lobes while a nominal time-independent stress (P) is applied to the right edge of the specimen shown in Fig. 1. Further details can be found in Ref. [48].

Effect of nominal stress

The effect of the mean applied nominal stress on the logarithmic CCM fatigue lifetime is illustrated in Fig. 5. Two different types of cyclic loadings were simulated: temperature cycling between 23 °C and 70 °C at constant 50% RH and humidity cycling between 50% and 90% RH at constant 23 °C temperature. The obtained fatigue lifetimes were analyzed at Points B and C along the centreline of the specimen rather than at the magnified stress points at the edge in order to provide generalized insight into the fatigue process. As expected, increasing the nominal stress causes a lower fatigue lifetime for the CCM material. Both locations on the specimen appear to withstand higher nominal stress under humidity cycling than under temperature cycling. The CCM fatigue lifetime is also shown to be more sensitive to the nominal stress than the corresponding fatigue lifetime of the pure membrane [48]. This can be explained by the fact that the catalyst layers are porous materials of lower stiffness than the membrane [55]. Hence, the main load bearing part of the CCM is believed to be the membrane due to which any reduction in the nominal stress is directly translated to a substantial increase in the CCM fatigue lifetime.

From Fig. 5, it is also observed that the two fatigue curves for temperature cycling are crossing each other at approximately 2 MPa nominal stress. Above this stress, the fatigue lifetime at Point C is higher than at Point B, while below this stress, the lifetime is higher at Point B. In contrast, under humidity cycling, the fatigue lifetime at Point C is consistently higher than at Point B. These differences are further analyzed by the time-dependent strain profiles under temperature and humidity cycling at these points, as presented in Fig. 6. The corresponding numerical data are also provided in Tables 3 and 4. For temperature cycling under 6 MPa nominal stress, the mean strain at Point B is considerably higher than at Point C (Fig. 6 and Table 3) which results in a somewhat lower

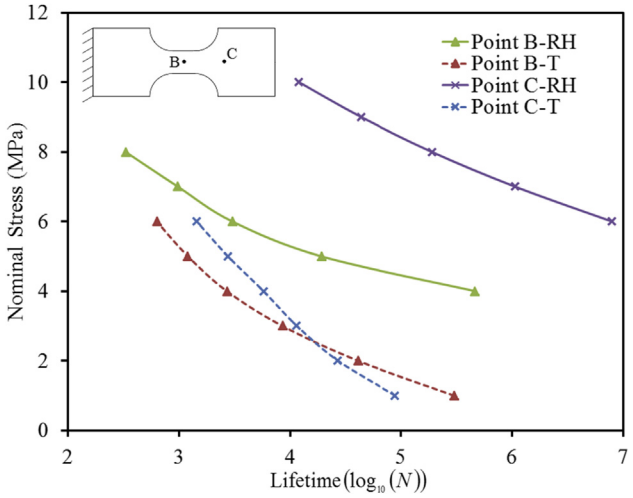

Fig. 5 – Simulated logarithmic CCM fatigue lifetime as a function of the mean applied nominal stress when the specimen is subjected to cyclic hygrothermal loadings based on isolated temperature (T) and relative humidity (RH) swings. The results were taken at Points B and C of the specimen geometry shown in the insert. The lifetime values given by the number of stress cycles until failure (N) are presented on a logarithmic scale.

lifetime. However, the fatigue lifetimes at these points are roughly the same, which indicates a marginal effect of the mean strain in relation to the strain amplitude. This is confirmed by the reversed lifetime effect at low nominal stress (1 MPa): here, the mean strain at Points B and C is almost identical, and the lower lifetime at Point C is attributed to its higher strain amplitude compared to Point B. The same behavior was also noted for the case of a pure membrane [48]. On the other hand, a combination of high mean strain and high strain amplitude results in a significantly reduced fatigue lifetime. At Point B, for instance, the fatigue lifetime under 6 MPa is significantly lower than under 1 MPa due to higher mean strain and higher amplitude of oscillation. For humidity cycling (Fig. 6 and Table 4), both the mean strain and strain amplitude at Point B are always higher than at Point C, which leads to a consistently lower lifetime. Overall, however, the strain amplitude is expected to be more influential than the mean strain.

Effects of temperature and humidity amplitudes

The effects of the amplitudes of the cyclic temperature and relative humidity loadings on the CCM fatigue lifetime are investigated based on the simulated results presented in Fig. 7 for two different nominal stresses in each case. Similar to the previous observations for a pure membrane [48], the CCM fatigue lifetime increases dramatically as the amplitude of the cyclic temperature or humidity loading decreases. In most cases, even a small 5 °C or 5% RH change in amplitude can lead to more than an order of magnitude difference in lifetime. The fatigue process is consistently more severe at Point B than at Point C due to the higher mean strain and strain amplitude at the narrow, central section of the specimen. For temperature cycling, amplitudes of at least 10 °C are required to induce

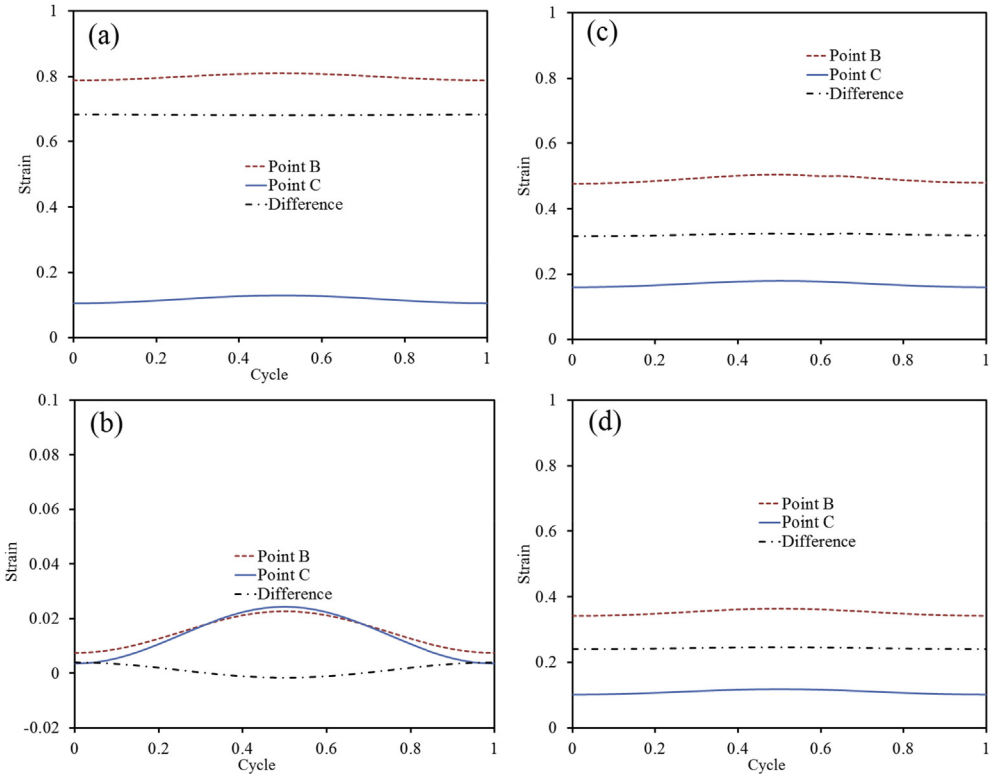

Fig. 6 – Time-dependent strain profiles at Points B and C under temperature cycling with nominal stress of (a) 6 MPa and (b) 1 MPa and under humidity cycling with a nominal stress of (c) 8 MPa and (d) 6 MPa. The horizontal axis represents the fraction of temperature cycle (a and b) and humidity cycle (c and d) completion.

Table 3 – Comparison of the amplitude and mean value of the strain oscillations and the corresponding fatigue lifetime (logarithmic) at Points B and C during temperature cycling at two different nominal stress levels.

	Point B			Point C		
	Amplitude	Mean	Lifetime	Amplitude	Mean	Lifetime
P = 6 MPa	1.08%	79.8%	2.80	1.20%	11.7%	3.16
P = 1 MPa	0.76%	1.5%	5.48	1.04%	1.3%	4.95

Table 4 – Comparison of the amplitude and mean value of the strain oscillations and the corresponding fatigue lifetime (logarithmic) at Points B and C during humidity cycling at two different nominal stress levels.

	Point B			Point C		
	Amplitude	Mean	Lifetime	Amplitude	Mean	Lifetime
P = 8 MPa	1.39%	48.9%	2.52	0.98%	16.9%	5.28
P = 6 MPa	1.12%	35.1%	3.48	0.84%	10.9%	6.9

measurable fatigue and amplitudes above ~20 °C result in severe fatigue. Similarly for humidity cycling, a minimum amplitude of 10% RH is required for measureable fatigue. In this case, however, the results are more intimately linked to the nominal stress and position within the specimen, and severe fatigue is only encountered for concurrently high levels of multiple factors. When compared to the previously reported fatigue results for the pure membrane [47,48], the CCM fatigue process during temperature cycling is much more severe, and may lead to an order of magnitude more rapid failures. In contrast, the fatigue process during humidity cycling appears to be more similar for the two materials, and is even found to be less severe in the CCM than in the membrane under certain conditions. The catalyst layers have been shown to reinforce the membrane against humidity induced expansion [46,55] thereby reducing the stress/strain amplitudes that develop within the CCM during humidity cycling and consequently resulting in longer CCM lifetime than for the pure membrane. In contrast, the catalyst layers tend to increase the thermal expansion of the CCM [16,20] and may therefore create a higher state of strain amplitude during temperature cycling than during humidity cycling.

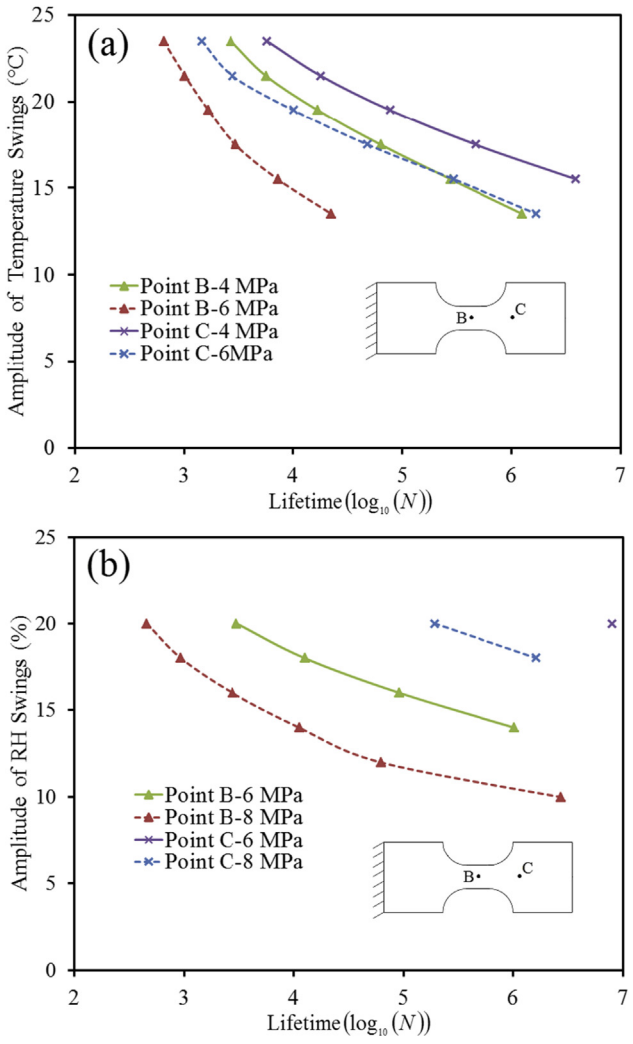

Fig. 7 – Simulated CCM fatigue lifetime when subjected to (a) temperature and (b) humidity cycling, shown as a function of the amplitude of the temperature and relative humidity oscillations at two different nominal stress levels (as indicated). The lifetime values given by the number of stress cycles until failure (N) are presented on a logarithmic scale.

Fatigue simulations under combined temperature and humidity loading

The actual temperature and humidity levels experienced by the CCM during in-situ fuel cell operation are likely to change concurrently, for instance during dynamic load changes between high and low power and during start-up/shutdown events. Hence, the present fatigue lifetime simulations were repeated for the case of simultaneous temperature and relative humidity cycles between (23 °C, 50% RH) and (70 °C, 90% RH). The simulated results obtained for two different levels of nominal stress are provided in Fig. 8. In the case of low nominal stress (0.1 MPa), the most critical points of the specimen are in the rectangular end lobes. This is due to the negligible mean stress and the presence of physical constraints in the rectangular sections that are ultimately translated into higher strain amplitudes at Point C. At a higher nominal stress, however, the fatigue-induced failure is predicted to occur at the edge of the central section of the specimen, similar to the previous findings. When compared to the findings of the previous section, the fatigue lifetime under combined temperature and humidity loadings is several orders of magnitude lower than that under isolated temperature or relative humidity loading, resulting in fatigue failures after merely ~100 to ~1000 cycles despite a much lower nominal stress. This is a consequence of the exacerbated strain amplitudes induced by the combined temperature and humidity cycles. Compared to the results for the pure membrane [48], the CCM simulations indicate slightly higher fatigue lifetime for the case of low nominal stress. However, due to the higher sensitivity of the CCM to the nominal stress, the fatigue lifetime of the CCM is lower than that of the pure membrane for the case of a higher mean stress.

Conclusions

An ex-situ tensile fatigue experiment was developed and utilized to explore the mechanical stability of catalyst coated membranes (CCMs) under a range of applied stress profiles and environmental conditions. A statistical design of experiment approach was employed to determine the effects of temperature and relative humidity on the maximum stress and associated fatigue lifetimes. A finite element based model was developed using the Smith-Watson-Topper (SWT) relationship to investigate the ex-situ fatigue lifetimes of CCM materials exposed to cyclic loadings. These types of loadings included both individual and combined cyclic temperature and relative humidity loadings.

It was found that the CCM fatigue lifetime decreases exponentially as the applied maximum stress is increased. At a given lifetime, the maximum tolerable stress level was

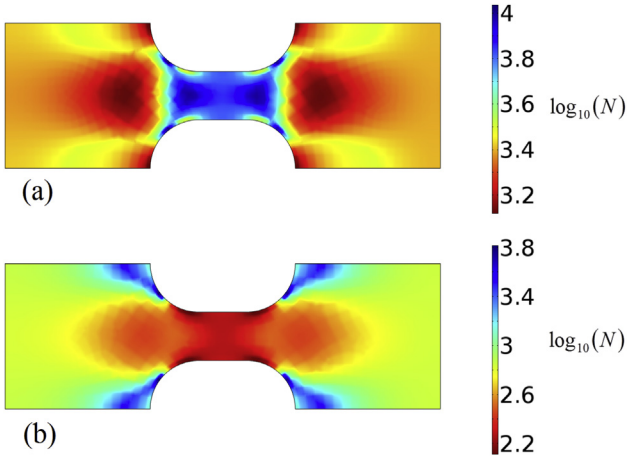

Fig. 8 – Spatial distribution of simulated fatigue lifetime within CCM specimen under cyclic hygrothermal loading conditions between (23 °C, 50% RH) and (70 °C, 90% RH) at nominal stress levels of (a) 0.1 MPa and (b) 1.0 MPa. The lifetime values given by the number of stress cycles until failure (N) are presented on a logarithmic scale. Lifetimes exceeding 10^7 cycles are not shown.

observed to drop at elevated levels of relative humidity and temperature due to the softening effect of the material at such environmental conditions. The effect of temperature was greater than that of relative humidity. Interestingly, the maximum tolerable stress level of the CCM material before the final rupture was significantly lower than that of the pure membrane, which is attributed to initial failure of the catalyst layers and stress transfer to the membrane.

ANOVA analysis of the experimental results revealed that the environmental conditions have negative main effects on the maximum tolerable stress level. However, the main effects of temperature and relative humidity were less significant than for the pure membrane, which is attributed to the lower post yield tangent modulus of the CCM material. Owing to the increased stiffness of the CCM, the interaction between temperature and relative humidity had a positive effect on the maximum stress levels. Furthermore, the strain to failure of the CCM was found to be lower than that of the pure membrane. This result confirms the confinement effect of the catalyst layers, but also reveals that the CCM may fail earlier than the membrane at a lower level of strain.

The developed finite element based model was first thoroughly validated against the experimental results and then applied to investigate CCM fatigue under hygrothermal cycling. The simulation results indicated that the CCM is more sensitive to the nominal stress than the pure membrane. This is attributed to the relatively weak nature of the catalyst layers which makes the membrane the main load bearing part of the CCM. Hence, any reduction in stress is translated into a profound increase in fatigue lifetime. Furthermore, it was discovered that the CCM fatigue lifetime increases dramatically with decreasing amplitude of the temperature and humidity cycles. The fatigue process during temperature cycling was more severe for the CCM than for the pure membrane due to higher strain amplitude resulting from the relatively high thermal expansion of the catalyst layers. In contrast, relative humidity cycles were less severe for the CCM material compared to the pure membrane. This is due to the reinforcement provided by the catalyst layers, which leads to a lower expansion amplitude during humidity loading. The simulations further revealed that combined temperature and humidity cycling can exacerbate the strain amplitude and reduce the fatigue lifetime by several orders of magnitude.

The ex-situ fatigue modeling approach presented in this work and based purely on the knowledge of material properties and failure criteria has so far been found to be valid for pure membrane and CCM materials and can be expected to be equally applicable to other similar materials such as mechanically reinforced membranes. This fatigue model could, therefore, prove to be of immense utility in the future of fuel cell durability research.

Acknowledgments

Funding for this research provided by the Natural Sciences and Engineering Research Council of Canada and Ballard Power Systems through an Automotive Partnership Canada grant is highly appreciated.

REFERENCES

[1] Wang Y, Chen KS, Mishler J, Cho SC, Adroher XC. A review of polymer electrolyte membrane fuel cells: technology, applications, and needs on fundamental research. Appl Energy 2011;88:981–1007. http://dx.doi.org/10.1016/j.apenergy.2010.09.030.

[2] Ahmadi P, Kjeang E. Comparative life cycle assessment of hydrogen fuel cell passenger vehicles in different Canadian provinces. Int J Hydrogen Energy 2015;40:12905–17. http://dx.doi.org/10.1016/j.ijhydene.2015.07.147.

[3] Gubler L, Koppenol WH. Kinetic simulation of the chemical stabilization mechanism in fuel cell membranes using cerium and manganese redox couples. J Electrochem Soc 2012;159. http://dx.doi.org/10.1149/2.075202jes. B211.

[4] Gubler L, Dockheer SM, Koppenol WH. Radical (HO•, H• and HOO•) formation and ionomer degradation in polymer electrolyte fuel cells. J Electrochem Soc 2011;158:B755–69. http://dx.doi.org/10.1149/1.3581040.

[5] Bosnjakovic A, Schlick S. Nafion perfluorinated membranes treated in fenton media: radical species detected by ESR spectroscopy. J Phys Chem B 2004;108:4332–7. http://dx.doi.org/10.1021/jp037519c.

[6] Ghassemzadeh L, Peckham TJ, Weissbach T, Luo X, Holdcroft S. Selective formation of hydrogen and hydroxyl radicals by electron beam irradiation and their reactivity with perfluorosulfonated acid ionomer. J Am Chem Soc 2013;135:15923–32.

[7] Macauley N, Ghassemzadeh L, Lim C, Watson M, Kolodziej J, Lauritzen M, et al. Pt band formation enhances the stability of fuel cell membranes. ECS Electrochem Lett 2013;2:F33–5.

[8] Macauley N, Sadeghi Alavijeh A, Watson M, Kolodziej J, Knights S, Wang G, et al. Accelerated membrane durability testing of heavy duty fuel cells. J Electrochem Soc 2015;162:F98–107.

[9] Patil YP, Jarrett WL, Mauritz KA. Deterioration of mechanical properties: a cause for fuel cell membrane failure. J Memb Sci 2010;356:7–13. http://dx.doi.org/10.1016/j.memsci.2010.02.060.

[10] Marrony M, Barrera R, Quenet S, Ginocchio S, Montelatici L, Aslanides A. Durability study and lifetime prediction of baseline proton exchange membrane fuel cell under severe operating conditions. J Power Sources 2008;182:469–75. http://dx.doi.org/10.1016/j.jpowsour.2008.02.096.

[11] Zhang S, Yuan X, Wang H, Merida W, Zhu H, Shen J, et al. A review of accelerated stress tests of MEA durability in PEM fuel cells. Int J Hydrogen Energy 2009;34:388–404. http://dx.doi.org/10.1016/j.ijhydene.2008.10.012.

[12] Wong KH, Kjeang E. Mitigation of chemical membrane degradation in fuel cells: understanding the effect of cell voltage and iron ion redox cycle. ChemSusChem 2015;8:1072–82. http://dx.doi.org/10.1002/cssc.201402957.

[13] Wong KH, Kjeang E. Macroscopic in-situ modeling of chemical membrane degradation in polymer electrolyte fuel cells. J Electrochem Soc 2014;161:F823–32.

[14] Tang H, Peikang S, Jiang SP, Wang F, Pan M. A degradation study of Nafion proton exchange membrane of PEM fuel cells. J Power Sources 2007;170:85–92. http://dx.doi.org/10.1016/j.jpowsour.2007.03.061.

[15] Andisheh-Tadbir M, Desouza A, Bahrami M, Kjeang E. Cell level modeling of the hygrothermal characteristics of open cathode polymer electrolyte membrane fuel cells. Int J Hydrogen Energy 2014;39:14993–5004. http://dx.doi.org/10.1016/j.ijhydene.2014.07.049.

[16] Silberstein MN, Boyce MC. Constitutive modeling of the rate, temperature, and hydration dependent deformation response of Nafion to monotonic and cyclic loading. J Power

Sources 2010;195:5692–706. http://dx.doi.org/10.1016/j.jpowsour.2010.03.047.
[17] Silberstein MN, Pillai PV, Boyce MC. Biaxial elastic–viscoplastic behavior of Nafion membranes. Polym Guildf 2011;52:529–39. http://dx.doi.org/10.1016/j.polymer.2010.11.032.
[18] Tang Y, Karlsson AM, Santare MH, Gilbert M, Cleghorn S, Johnson WB. An experimental investigation of humidity and temperature effects on the mechanical properties of perfluorosulfonic acid membrane. Mater Sci Eng A 2006;425:297–304. http://dx.doi.org/10.1016/j.msea.2006.03.055.
[19] Beuscher U, Cleghorn SJC, Johnson WB. Challenges for PEM fuel cell membranes. Int J Energy Res 2005;29:1103–12. http://dx.doi.org/10.1002/er.1142.
[20] Sadeghi Alavijeh A, Goulet M-A, Khorsany R, Ghataurah J, Lim C, Lauritzen M, et al. Decay in mechanical properties of catalyst coated membranes subjected to combined chemical and mechanical membrane degradation. Fuel Cells 2015;15:204–13.
[21] Alavijeh AS, Khorasany RMH, Nunn Z, Habisch A, Lauritzen M, Rogers E, et al. Microstructural and mechanical characterization of catalyst coated membranes subjected to in situ hygrothermal fatigue. J Electrochem Soc 2015;162:1461–9. http://dx.doi.org/10.1149/2.0471514jes.
[22] Solasi R, Zou Y, Huang X, Reifsnider K. A time and hydration dependent viscoplastic model for polyelectrolyte membranes in fuel cells. Mech Time-Dependent Mater 2008;12:15–30. http://dx.doi.org/10.1007/s11043-007-9040-7.
[23] Kusoglu A, Karlsson AM, Santare MH, Cleghorn S, Johnson WB. Mechanical behavior of fuel cell membranes under humidity cycles and effect of swelling anisotropy on the fatigue stresses. J Power Sources 2007;170:345–58. http://dx.doi.org/10.1016/j.jpowsour.2007.03.063.
[24] Khattra NS, Karlsson AM, Santare MH, Walsh P, Busby FC. Effect of time-dependent material properties on the mechanical behavior of PFSA membranes subjected to humidity cycling. J Power Sources 2012;214:365–76. http://dx.doi.org/10.1016/j.jpowsour.2012.04.065.
[25] Kusoglu A, Tang Y, Lugo M, Karlsson AM, Santare MH, Cleghorn S, et al. Constitutive response and mechanical properties of PFSA membranes in liquid water. J Power Sources 2010;195:483–92. http://dx.doi.org/10.1016/j.jpowsour.2009.08.010.
[26] Silberstein MN, Boyce MC. Hygro-thermal mechanical behavior of Nafion during constrained swelling. J Power Sources 2011;196:3452–60.
[27] Yoon W, Huang X. A nonlinear viscoelastic–viscoplastic constitutive model for ionomer membranes in polymer electrolyte membrane fuel cells. J Power Sources 2011;196:3933–41. http://dx.doi.org/10.1016/j.jpowsour.2010.12.034.
[28] García-Salaberri PA, Vera M, Zaera R. Nonlinear orthotropic model of the inhomogeneous assembly compression of PEM fuel cell gas diffusion layers. Int J Hydrogen Energy 2011;36:11856–70. http://dx.doi.org/10.1016/j.ijhydene.2011.05.152.
[29] Carral C, Mélé P. A numerical analysis of PEMFC stack assembly through a 3D finite element model. Int J Hydrogen Energy 2014;39:4516–30. http://dx.doi.org/10.1016/j.ijhydene.2014.01.036.
[30] Oh K, Chippar P, Ju H. Numerical study of thermal stresses in high-temperature proton exchange membrane fuel cell (HT-PEMFC). Int J Hydrogen Energy 2013:1–10. http://dx.doi.org/10.1016/j.ijhydene.2013.01.201.
[31] Zhou Y, Lin G, Shih AJ, Hu SJ. Assembly pressure and membrane swelling in PEM fuel cells. J Power Sources 2009;192:544–51. http://dx.doi.org/10.1016/j.jpowsour.2009.01.085.
[32] Poornesh KK, Sohn Y-J, Park G-G, Yang T-H. Gas-diffusion layer's structural anisotropy induced localized instability of nafion membrane in polymer electrolyte fuel cell. Int J Hydrogen Energy 2012;37:15339–49. http://dx.doi.org/10.1016/j.ijhydene.2012.04.154.
[33] Khorasany RMH, Goulet MA, Sadeghi Alavijeh A, Kjeang E, Wang GG, Rajapakse RKND. On the constitutive relations for catalyst coated membrane applied to in-situ fuel cell modeling. J Power Sources 2014;252:176–88.
[34] Solasi R, Zou Y, Huang X, Reifsnider K, Condit D. On mechanical behavior and in-plane modeling of constrained PEM fuel cell membranes subjected to hydration and temperature cycles. J Power Sources 2007;167:366–77. http://dx.doi.org/10.1016/j.jpowsour.2007.02.025.
[35] Bograchev D, Gueguen M, Grandidier J, Martemianov S. Stress and plastic deformation of MEA in running fuel cell. Int J Hydrogen Energy 2008;33:5703–17. http://dx.doi.org/10.1016/j.ijhydene.2008.06.066.
[36] Sadeghi Alavijeh A, Khorasany RMH, Habisch A, Wang GG, Kjeang E. Creep properties of catalyst coated membrane in polymer electrolyte fuel cells. J Power Sources 2015;285:16–28.
[37] Sadeghi Alavijeh A, Venkatesan SV, Khorasany RMH, Kim WHJ, Kjeang E. Ex-situ tensile fatigue-creep testing: a powerful tool to simulate in-situ mechanical degradation in fuel cells. J Power Sources 2016;312:123–7. http://dx.doi.org/10.1016/j.jpowsour.2016.02.053.
[38] Li Y, Quincy JK, Case SW, Ellis MW, Dillard DA, Lai Y-H, et al. Characterizing the fracture resistance of proton exchange membranes. J Power Sources 2008;185:374–80. http://dx.doi.org/10.1016/j.jpowsour.2008.06.056.
[39] Moukheiber E, Bas C, Flandin L. Understanding the formation of pinholes in PFSA membranes with the essential work of fracture (EWF). Int J Hydrogen Energy 2014;39:2717–23. http://dx.doi.org/10.1016/j.ijhydene.2013.03.031.
[40] Solasi R, Huang X, Reifsnider K. Creep and stress-rupture of Nafion® membranes under controlled environment. Mech Mater 2010;42:678–85. http://dx.doi.org/10.1016/j.mechmat.2010.04.005.
[41] Banan R, Bazylak A, Zu J. Effect of mechanical vibrations on damage propagation in polymer electrolyte membrane fuel cells. Int J Hydrogen Energy 2013;38:14764–72.
[42] Banan R, Bazylak A, Zu J. Combined effects of environmental vibrations and hygrothermal fatigue on mechanical damage in PEM fuel cells. Int J Hydrogen Energy 2015;40:1911–22.
[43] Lim C, Ghassemzadeh L, Van Hove F, Lauritzen M, Kolodziej J, Wang GG, et al. Membrane degradation during combined chemical and mechanical accelerated stress testing of PEM fuel cells. J Power Sources 2014;257:102–10. http://dx.doi.org/10.1016/j.jpowsour.2014.01.106.
[44] Lim C, Sadeghi Alavijeh A, Lauritzen M, Kolodziej J, Knights S, Kjeang E. Fuel cell durability enhancement with cerium oxide under combined chemical and mechanical membrane degradation. ECS Electrochem Lett 2015;4:F29–31.
[45] Kusoglu A, Weber AZ. A mechanistic model for pinhole growth in fuel-cell membranes during cyclic loads. J Electrochem Soc 2014;161:E3311–22. http://dx.doi.org/10.1149/2.036408jes.
[46] Goulet M, Arbour S, Lauritzen M, Kjeang E. Water sorption and expansion of an ionomer membrane constrained by fuel cell electrodes. J Power Sources 2015;274:94–100.
[47] Khorasany RMH, Sadeghi Alavijeh A, Kjeang E, Wang GG, Rajapakse RKND. Mechanical degradation of fuel cell membranes under fatigue fracture tests. J Power Sources 2015;274:1208–16. http://dx.doi.org/10.1016/j.jpowsour.2014.10.135.
[48] Khorasany RMH, Kjeang E, Wang GG, Rajapakse RKND. Simulation of ionomer membrane fatigue under mechanical and hygrothermal loading conditions. J Power Sources

2015;279:55–63. http://dx.doi.org/10.1016/j.jpowsour.2014.12.133.
[49] Aindow TT, O'Neill J. Use of mechanical tests to predict durability of polymer fuel cell membranes under humidity cycling. J Power Sources 2011;196:3851–4.
[50] Pestrak M, Li Y, Case SW, Dillard DA, Ellis MW, Lai Y-H, et al. The effect of mechanical fatigue on the lifetimes of membrane electrode assemblies. J Fuel Cell Sci Technol 2010;7:041009. http://dx.doi.org/10.1115/1.4000629.
[51] Huang X, Solasi R, Zou YUE, Feshler M, Reifsnider K, Condit D, et al. Mechanical Endurance of polymer electrolyte membrane and PEM fuel cell durability. J Polym Sci Part B Polym Phys 2006;44:2346–57. http://dx.doi.org/10.1002/polb.
[52] Shi S, Chen G, Wang Z, Chen X. Mechanical properties of Nafion 212 proton exchange membrane subjected to hygrothermal aging. J Power Sources 2013;238:318–23. http://dx.doi.org/10.1016/j.jpowsour.2013.03.042.
[53] Burlatsky SF, Gummalla M, O'Neill J, Atrazhev VV, Varyukhin AN, Dmitriev DV, et al. A mathematical model for predicting the life of polymer electrolyte fuel cell membranes subjected to hydration cycling. J Power Sources 2012;215:135–44. http://dx.doi.org/10.1016/j.jpowsour.2012.05.005.
[54] Kusoglu A, Santare MH, Karlsson AM. Aspects of fatigue failure mechanisms in polymer fuel cell membranes. J Polym Sci Part B Polym Phys 2011;49:1506–17. http://dx.doi.org/10.1002/polb.22336.
[55] Goulet MA, Khorasany RMH, De Torres C, Lauritzen M, Kjeang E, Wang GG, et al. Mechanical properties of catalyst coated membranes for fuel cells. J Power Sources 2013;234:38–47. http://dx.doi.org/10.1016/j.jpowsour.2013.01.128.
[56] Jia R, Dong S, Hasegawa T, Ye J, Dauskardt RH. Contamination and moisture absorption effects on the mechanical properties of catalyst coated membranes in PEM fuel cells. Int J Hydrogen Energy 2012;37:6790–7. http://dx.doi.org/10.1016/j.ijhydene.2012.01.063.
[57] Uchiyama T, Kumei H, Yoshida T. Catalyst layer cracks by buckling deformation of membrane electrode assemblies under humidity cycles and mitigation methods. J Power Sources 2013;238:403–12. http://dx.doi.org/10.1016/j.jpowsour.2013.04.026.
[58] Khattra NS, Lu Z, Karlsson AM, Santare MH, Busby FC, Schmiedel T. Time-dependent mechanical response of a composite PFSA membrane. J Power Sources 2013;228:256–69. http://dx.doi.org/10.1016/j.jpowsour.2012.11.116.
[59] Lu Z, Kim C, Karlsson AM, Cross JC, Santare MH. Effect of gas diffusion layer modulus and land–groove geometry on membrane stresses in proton exchange membrane fuel cells. J Power Sources 2011;196:4646–54. http://dx.doi.org/10.1016/j.jpowsour.2011.01.028.
[60] Lai Y-H, Mittelsteadt CK, Gittleman CS, Dillard DA. Viscoelastic stress analysis of constrained proton exchange membranes under humidity cycling. J Fuel Cell Sci Technol 2009;6:021002. http://dx.doi.org/10.1115/1.2971045.
[61] Sadeghi Alavijeh A, Khorasany RMH, Habisch A, Wang GG, Kjeang E. Creep properties of catalyst coated membranes for polymer electrolyte fuel cells. J Power Sources 2015;285:16–28. http://dx.doi.org/10.1016/j.jpowsour.2015.03.082.
[62] Lykins CD, Mall S, Jain V. An evaluation of parameters for predicting fretting fatigue crack initiation. Int J Fatigue 2000;22:703–16.
[63] Ince A, Glinka G. A modification of Morrow and Smith-Watson-Topper mean stress correction models. Fatigue Fract Eng Mater Struct 2011;34:854–67. http://dx.doi.org/10.1111/j.1460-2695.2011.01577.x.
[64] Sum W, Williams E, Leen S. Finite element, critical-plane, fatigue life prediction of simple and complex contact configurations. Int J Fatigue 2005;27:403–16. http://dx.doi.org/10.1016/j.ijfatigue.2004.08.001.